

# Antennal morphology as a physical filter of olfaction: temporal tuning of the antennae of the honeybee, *Apis mellifera*

Robb W.S. Schneider, Brad A. Price, Paul A. Moore \*

Laboratory for Sensory Ecology, Department of Biological Sciences, Bowling Green State University, Bowling Green, Ohio, 43403, USA

Received 13 June 1997; received in revised form 29 October 1997

## Abstract

There are many different antennal morphologies for insects, yet they all have the same functional role in olfaction. Chemical signals are dispersed through two physical forces; diffusion and fluid flow. The interaction between antennal morphology and fluid flow generates a region of changing flow velocity called the boundary layer. The boundary layer determines signal dispersion dynamics and therefore influences the signal structure and information that arrives at the receptor cells. To investigate how the boundary layer changes the information in the signals arriving at receptor cells, we measured chemical dynamics within the boundary layer around the bee antennae using microelectrodes. We used two types of chemical signals: pulsed and continuous. The results showed that the boundary layer increased the decay time of the chemical signal for the pulsatile stimuli and increased the peak height for the continuous data. Spectral analysis of continuous signals showed that the temporal aspects of the chemical signal are changed by the boundary layer. Particularly the temporal dynamics of the signal are dampened at the slowest flow speed and amplified at the intermediate and fast flow speeds. By altering the structure of the chemical signal, the morphology will function as a sensory filter. © 1998 Elsevier Science Ltd. All rights reserved.

**Keywords:** Antenna; *A. mellifera*; Chemoreception; Fluid flow; Olfaction

## 1. Introduction

The insect world has many different antennae morphologies. At one end of the morphological spectrum, there is the highly complex pectinate structure, which is branched and has a large surface area, as in the moth (*Actias luna*) (Borror et al., 1989). At the other end of the spectrum is the relatively simple geniculate-like structure that has a dimpled surface as in the honeybee (*Apis mellifera*) (Borror et al., 1989). Although immense diversity is seen in the antennal morphology of insects, they all serve the same function in chemoreception, which is to enhance the detection of molecules from the environment.

In chemoreception, the dispersion of the signal is distributed by two physical processes; fluid flow (Vogel, 1983) and molecular diffusion (DeSimone, 1981; Futrelle, 1984). The relationship between these two

physical processes in the dispersion of chemical signals is described by the Peclet number (Pe). In environments with Pe numbers greater than one, flow is the dominant physical dispersal mechanism and in situations with Pe numbers less than one, molecular diffusion is the dominant force.

At macroscopic scales, the dispersion of chemical signals is dominated by flow, which is usually turbulent. Turbulent forces determine the magnitude of fluctuations that occur within an odor plume, and thus determine the temporal nature of signals that are available for the animals to use for information. Odor plumes generated under different turbulence regimes will have different chemical fluctuations (i.e. spatial and temporal profile of a chemical signal, Moore et al., 1994; Murlis et al., 1991). These fluctuations in concentration and patchiness of the distribution constitute a part of the information within a chemical signal.

The information contained within a chemical signal has been described as having four aspects; quality, intensity, spatial and temporal distribution (Ache, 1988). Dispersal forces in a given flow regime affect the latter three

\* Corresponding author. Tel.: + 1-419-372-8556; Fax: + 1-419-372-2024; E-mail: pmoore@bgnnet.bgsu.edu

parameters of the chemical signal. Therefore any change in these physical forces or their ratio during dispersion will change the information contained within a chemical signal.

Antennae morphology plays a critical role in modifying the flow patterns. As fluid flows over a solid surface such as in insect antennae, the fluid 'layer' in direct contact with the surface does not flow (the no-slip condition, Vogel, 1994). In this region, there is a velocity gradient where the fluid velocity is zero at the surface, and extends out from the solid to 95% of the freestream velocity (Schlichting, 1987). This region of reduced flow around the solid surface (e.g. antenna) is referred to as the boundary layer. As the velocity changes within the boundary layer, the dynamics of signal dispersion also changes. There is a change from flow-dominated dispersion away from the antenna to diffusion-dominated dispersion near the antenna.

By altering the dynamics of signal dispersion, the boundary layer will change the chemical signal structure. This change in structure affects the information contained in the chemical signal, acting as a sensory filter by altering the information of chemical signals arriving at the receptor cells (Moore et al., 1991; Schneider et al., 1997). Since the spatial and temporal structure of the chemical signals are determined by the interaction between fluid flow and molecular diffusion, the boundary layer can have a profound affect on the chemical signal structure.

Previous work on flow through sensory appendages has shown that changes in flow velocity and hair spacing can dramatically alter flow patterns (Cheer and Koehl, 1987; Koehl, 1993, 1995, 1996) and that these changes in flow patterns can alter chemical signal dynamics (Moore et al., 1992). Schneider et al., 1997 found that the boundary layer around a moth's (*Manduca sexta*), antennae changes different aspects of the chemical signal. Particularly the flux of chemicals, signal onset and decay time of the chemical signal were altered by the morphology of the antennae. Moore et al. (1992) also found that the boundary layer around the lateral antennule of the lobster (*Homarus americanus*), drastically affects the incoming chemical signal as it arrives to the receptor cell surface. Studies on the spiny lobster have produced similar results (Gleeson et al., 1993) As these studies show the boundary layer around chemoreceptive organs affects the incoming chemical signal. The change in dispersal forces due to the boundary layer acts as a physical filter on the incoming chemical signal.

In this study we measured tracer chemical dynamics in the boundary layer of the honeybee (*A. mellifera*) with microelectrodes to examine the effect that the boundary layer around a simplified antenna has on chemical signal structure arriving at receptor cells. This study is designed to look at the role the relatively simple antennal morphology of *A. mellifera* has on the chemical signal com-

ing into the local receptor environment. In comparison, a previous study by Schneider et al., 1997 looked at the effect of an elaborate antennal design that the male and female moth (*M. sexta*) had on the incoming chemical signal.

## 2. Materials and methods

### 2.1. Modeling air flow in a water medium

To use current electrochemical technology to measure chemical signals (IVEC-10), we used water instead of air as our medium of flow. Since air and water are both fluids, either can be used to model fluid flow if the flow dynamics are the same for each medium (Vogel, 1983, 1994). The patterns of flow in a system can be described by the Reynolds number ( $Re = \mathbf{u}l/\nu$ ), where  $\mathbf{u}$  is the relative velocity,  $l$  is a characteristic length scale, and  $\nu$  is kinematic viscosity of the fluid. If the Reynolds number of an antenna in air is identical to the  $Re$  number of an antenna in water, then the flow patterns of both situations are identical and water can be used to model flow in air (Vogel, 1983, 1994).

We have taken the diameter of the antennae ( $2.1 \times 10^{-4}$  m) as the characteristic length scale and the kinematic viscosity of air was  $1.5 \times 10^{-5}$  m<sup>2</sup> s<sup>-1</sup> at 20°C. Typical flight speeds for *A. mellifera* workers ranged from 1.5 m s<sup>-1</sup> to 3.5 m s<sup>-1</sup> (Nachtigall and Hanauer-Thieser, 1992). Thus, the antennae on a flying worker bee have a  $Re$  number of 21 at 1.5 m s<sup>-1</sup>, 35 at 2.5 m s<sup>-1</sup>, and 49 at 3.5 m s<sup>-1</sup> respectively.

To equate both the flow patterns and forces of an antenna in air to an antenna in water, Vogel (1983) used a 28-fold reduction of velocities in water and an increase in temperature to 52°C. Consequently, we used water velocities of 0.05, 0.09 and 0.12 m s<sup>-1</sup> to correspond to the air speeds of 1.5, 2.5 and 3.5 m s<sup>-1</sup>, respectively.

It was also necessary to match the chemical dispersion dynamics of a system in air to a system in water. The Peclet number indicates the relative contribution of fluid flow and molecular diffusion in chemical dispersion ( $Pe = \mathbf{u}l/D_m$ ), where  $\mathbf{u}$  is the relative velocity,  $l$  is a characteristic length scale, and  $D_m$  is the diffusion coefficient. For  $D_m$ , we have taken the diffusion coefficient of bombykol (0.025 cm<sup>2</sup> s<sup>-1</sup>; Adam and Delbrück, 1968). The relative velocity and characteristic length scale were identical to those used above. Using these values, we calculate a  $Pe$  number for a worker bee in air as 126 at 1.5 m s<sup>-1</sup>, 210 at 2.5 m s<sup>-1</sup> and 294 at 3.5 m s<sup>-1</sup>. The electrochemical detection system used dopamine as the tracer molecule, which has a diffusion coefficient of  $2 \times 10^{-9}$  m<sup>2</sup> s<sup>-1</sup> in 20°C water. To approximate the dispersion dynamics (and  $Pe$  number) of a bee antennae in air with one in water, we increased the temperature of the water as stated above. The diffusion coefficient of the

molecule changes with temperature according to the relationship  $D_m = T \cdot f$  (Adamson, 1973).  $f$  is a function that describes the relationship between temperature and diffusion. The diffusion coefficient of dopamine is  $2 \times 10^{-9} \text{ m}^2 \text{ s}^{-1}$  at 293 K. By increasing the temperature 32 K to 325 K, the diffusion coefficient of dopamine increased to  $2.2 \times 10^{-9} \text{ m}^2 \text{ s}^{-1}$ . Under these conditions, the Peclet numbers of the bee antennae in water were 4772, 8590, 11 454 at  $0.05 \text{ m s}^{-1}$ ,  $0.09 \text{ m s}^{-1}$  and  $0.12 \text{ m s}^{-1}$ , respectively. While the Peclet numbers in water were an order of magnitude greater ( $\approx 40$ -fold) than those in air, both situations indicate a flow-dominated dispersion system. The temporal dynamics of signals recorded during these larger Peclet conditions will be slightly higher in frequency than normally encountered by the antennae.

## 2.2. Animals and flow tank

Dr E. Erickson of the USDA-ARS PWA Carl Hayden HoneyBee Research Center (Tucson, Arizona) provided the bees. The animals were live-caught (9.25.96) and shipped in 95% ETOH. The animals used had an antennal diameter of  $2.1 \times 10^{-4} \pm 2 \times 10^{-5} \text{ m}$  (mean  $\pm$  S.E.M.).

The experiment was conducted in a recirculating flow tank ( $0.13 \text{ m} \times 0.14 \text{ m} \times 0.90 \text{ m}$ ) constructed with 4 inch PVC pipe (see Fig. 1 in Schneider et al., 1997). The odor source was delivered from a Pasteur pipette 8 cm up-current from the antennae and electrode for the continuous and pulse odor signals. Water was obtained from a hot water tap adjusted to  $52^\circ\text{C} \pm 1^\circ\text{C}$ . The flow tank was drained and refilled after each trial. To maintain the flow tank at  $52^\circ\text{C}$ , Tygon<sup>®</sup> tubing (1.27 cm ID) was wrapped around the return pipe and hot water was circulated through it. The odor signal was stored in a water bath at  $52^\circ\text{C}$  to ensure the water in the flow tank and odor signal were at the same temperature. Flow speeds were

controlled with an electric motor (Security Universal<sup>®</sup> model # U-116) with a 4-blade prop (blades  $45^\circ$  normal to the shaft), and a variable transformer (Staco Energy<sup>®</sup> model # 3PN1010). Flow speeds were determined by averaging twenty neutrally buoyant particle velocities at set transformer voltages.

A single *A. mellifera* head and thorax were held in place with a 28 gauge needle. The needle pierced through the thorax normal to flow. The legs and abdomen were cut off each subject. The needle and honeybee were mounted onto a micromanipulator (Stoelting MM 33) to move the antennae to the fixed recording electrode in the working section of the flow tank. The electrode tip was placed on the surface of the right antennae at an angle of  $55^\circ$  (Fig. 1).

## 2.3. Recording techniques

Since the introduction of micro-electrochemical techniques, developed to record neurotransmitter concentrations within the CNS tissue (Gerhardt et al., 1984, 1987), to aquatic applications, it has become possible to quantify chemical distributions at biologically relevant spatial scales and with high temporal resolution (Moore and Atema, 1991; Moore et al., 1989, 1991, 1992, 1994). The IVEC-10 recording technique is now a standard practice for these applications and has been used in studies similar to the present study to measure chemical dynamics within other sensory appendages (Moore et al., 1989, 1991; Schneider et al., 1997). This technique has several advantages for chemosensory applications: which include small electrode sizes (diameters of 30 microns to 150 microns) comparable to receptor hair dimensions, fast temporal sampling (up to 200 Hz), and the ability to place electrodes within sensory structures without compromising electrode operation (Moore et al., 1989).

Recordings were made at a sampling rate of 10 Hz using the IVEC-10 (In Vivo Electrochemistry Computer System; Medical Systems Corp., Greenvale, NY). Each 100 ms epoch for the 10 Hz sampling rate was composed of a 50 ms epoch at  $+0.55 \text{ v}$  (oxidation) followed by a 50 ms epoch at  $0.0 \text{ v}$  (reduction). The recording electrodes were sampled every 50 ms with analog-to-digital conversions of the samples occurring at 4 kHz. These data were averaged for the 50 ms time epoch. Further details of recording and digitizing are explained elsewhere (Moore et al., 1989).

The electrodes were composed of a 30 micron diameter carbon fiber and calibrated in solutions of dopamine. Electrodes exhibited linearity over a concentration range of 0.5 to 100 micromolar (correlation coefficient;  $r^2 > 0.95$ ). The electrodes actually measure chemical flux in that they are detecting the number of molecular encounters with the electrode's surface per unit time. For the sake of simplicity, we use the term 'concentration' to

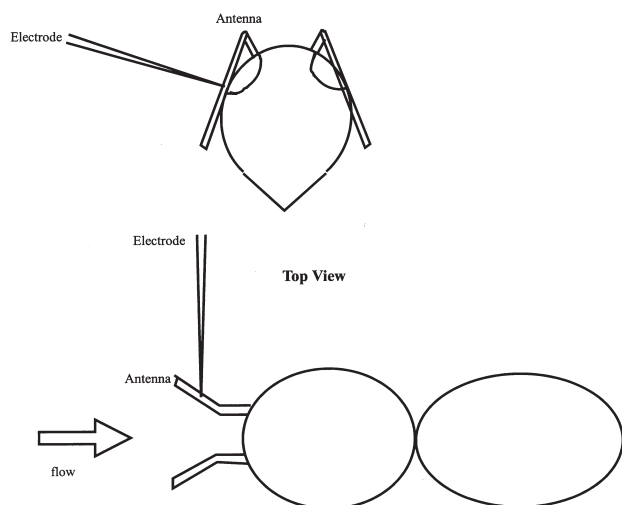


Fig. 1. The arrangement of the electrode on the antenna detailed.

describe the calibrated signal from the electrodes. A more accurate description in flowing systems may be 'molecular encounters per unit time' or chemical flux. Since chemoreceptors also integrate molecular events over some time unit, the electrodes and chemoreceptor cells detect chemicals in a similar manner.

Chemical signals for the continuous odor plumes and single odor pulses were measured at the middle of the antennae. In addition, the chemical signals were recorded at three different flow speeds:  $0.05 \pm 0.004 \text{ m s}^{-1}$ ,  $0.09 \pm 0.004 \text{ m s}^{-1}$ , and  $0.12 \pm 0.004 \text{ m s}^{-1}$ . Six bees were used in the experiment and were subjected to 6 min trials at each of the three flow speeds for the continuous odor plume and ten pulse signals.

The trials were done in a dark room with the antennae illuminated with a Dolan-Jenner Fiber Lite 1990. The trials were videorecorded with a Panasonic WV-CL350 camera, onto a Panasonic AG-1980 VCR displayed on a Sony PVM-1351Q trinitron video monitor.

#### 2.4. Chemical signal

The odor source was 4 mM dopamine, 2 mM ascorbic acid, and 0.05 mM fluorescein. The continuous odor signal was stored in a 1 l Pyrex reservoir connected to a Pasteur Pipette delivery system. The chemical signal was gravity fed at rate  $60 \text{ ml s}^{-1}$  into the center of the flume through an in-line flow meter (Manostat #2).

To deliver pulses, a small volume valve (General Valve 3-111-900) was controlled by a single output stimulator (Grass S48) which opened the valve for 350 milliseconds. Pulses were manually triggered after the previous pulse had been flushed from the boundary layer of the antennae by the flow as measured by IVEC. Ten pulses were recorded for each antennae and flow speed. Controls were measured by removing the antennae and measuring the odor signals with the electrode in the center of the working section under identical conditions, i.e. working distance, and electrode angle.

#### 2.5. Data analysis

Different aspects of the temporal profile of the chemical signal were analysed using a lab designed BASIC program. Signal parameters analysed included peak height, slope of the signal, peak length (Moore and Atema, 1988) and decay time of the signal (Schneider et al., 1997). These parameters were chosen as those most relevant to the encoding of information by sensory neurons (Borroni and Atema, 1988; Gomez et al., 1994). Further details on the other definitions and discussion of their relevance can be found in Moore et al. (1994). One-way ANOVA with Tukey-HSD post hoc test were used to determine differences between flow speeds within the control data. The *t*-tests were used to determine changes in pulse parameters between boundary layer and control.

All significant differences were determined using  $p < 0.05$ .

A spectral analysis was used to analyse the continuous data using the Fast Fourier Transform method by a commercial program (Statistica by Statsoft). The spectral analyses of the odor profiles were run on the three sequential 85 s intervals of the total 4.25 min. Subsequently, the three spectral analyses were averaged across the six bees, and normalized to the maximum value within the spectral analysis. This method resulted in the best estimate of the frequency spectrum, but also include some loss in frequency resolution (Moore, 1994; D. Mountain, pers. comm.). The frequency graphs were constructed by subtracting the experimental analysis results from the control spectral analysis. Thus the graphs were difference plots which indicated the aspects of the chemical signal that were amplified (positive values) or filtered (negative values) by the physical morphology.

### 3. Results

#### 3.1. Pulse signal

##### 3.1.1. Effect of flow on control pulses

For the control odor pulses, both the peak height and onset slope significantly decreased as flow velocity increased (Fig. 2; one-way ANOVA,  $p < 0.05$ ). Peak height decreased from  $7.6 \pm 0.3 \mu\text{M}$  (at  $0.05 \text{ m s}^{-1}$ ) to  $6.7 \pm 0.4 \mu\text{M}$  (at  $0.09 \text{ m s}^{-1}$ ) to  $6.0 \pm 0.3 \mu\text{M}$  (at  $0.12 \text{ m s}^{-1}$ ). ANOVAs showed that each of these means were significantly different from each other (one-way ANOVA,  $p < 0.05$ ). Onset slope decreased significantly from  $39.5 \pm 3.9 \mu\text{M s}^{-1}$  ( $0.05 \text{ m s}^{-1}$ ) to  $33.2 \pm 3.9 \mu\text{M s}^{-1}$  ( $0.09 \text{ m s}^{-1}$ ) to  $27.4 \pm 3.3 \mu\text{M s}^{-1}$  ( $0.12 \text{ m s}^{-1}$ ) (one-way ANOVA,  $p < 0.05$ ). There was a significant difference between the slope values of slowest flow speed compared to the intermediate and fast flow speeds. In addition, the decay time decreased significantly as the flow speed was increased. The decay time at the fastest flow speed ( $1.04 \pm 0.04 \text{ s}$ ) was significantly shorter than the decay times at the intermediate and slowest flow speeds ( $0.97 \pm 0.05 \text{ s}$  and  $0.75 \pm 0.04 \text{ s}$ , respectively; one-way ANOVA,  $p < 0.05$ ). The pulse shape was reduced in concentration and in slope, and decayed in a shorter period of time as the flow velocity was increased.

##### 3.1.2. Effect of worker bee antennae morphology on pulse signal parameters

The peak height was not significantly different for the antenna compared to control values (Fig. 2A; *t*-test,  $p > 0.05$ ). The onset slope was not significantly different within the boundary layer of the honeybee antennae at any of the speeds tested (Fig. 2B). The decay time was

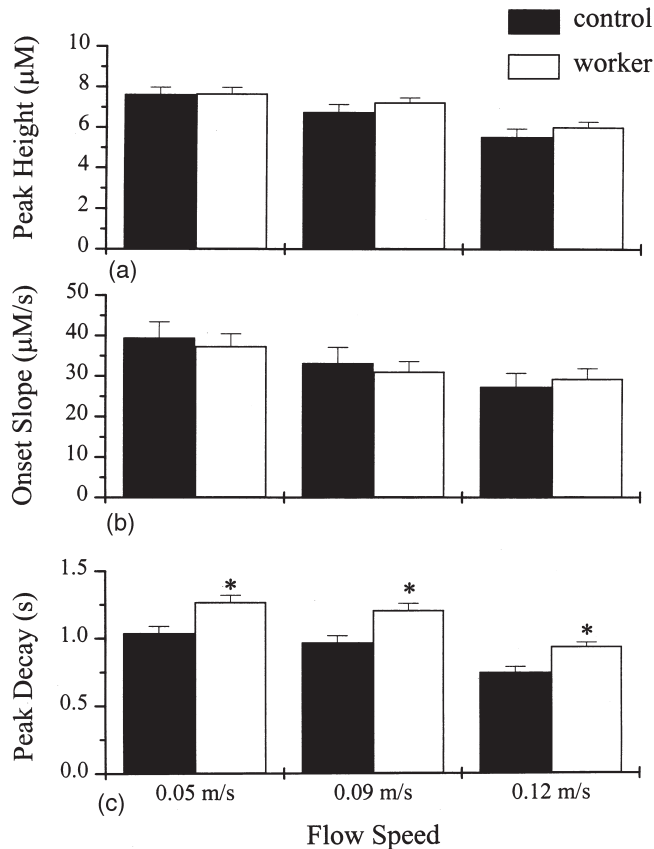


Fig. 2. Changes in pulse parameters in the boundary layer surrounding worker bee antennae at three different flow speeds for single pulses. (A) Peak for control (black bar), and worker bee antennae (white bar). (B) Onset slope for control (black bar), and worker bee antennae (white bar). (C) Decay time of the chemical signal for control (black bar), and worker bee antennae (white bar). Points represent mean ( $\pm$  S.E.M.) for 10 pulses each for six antennae. The  $t$ -tests were used to determine significant difference. Asterisk (\*) indicates significant differences when compared with control  $p < 0.05$  for all tests.

significantly longer within the boundary layer of the honeybee antennae than the decay time of the control plume for all three speeds (Fig. 2C). The boundary layer surrounding the worker antenna significantly increased the decay time as compared to control values.

### 3.2. Continuous signal

#### 3.2.1. Effect of flow on control odor plumes

The peak heights at the slowest and intermediate flow speed were significantly higher than the fastest flow speed (Fig. 3; one-way ANOVA,  $p < 0.05$ ). The onset slope significantly decreased as the flow speed was increased. Peak length for the fastest flow speed was significantly shorter than the slowest and intermediate flow speeds (one-way ANOVA,  $p < 0.05$ ).

#### 3.2.2. Effect of the honeybee antennae morphology on turbulent odor plume parameters

Within the micro-environment around the bee antennae, the peak height was significantly higher at the

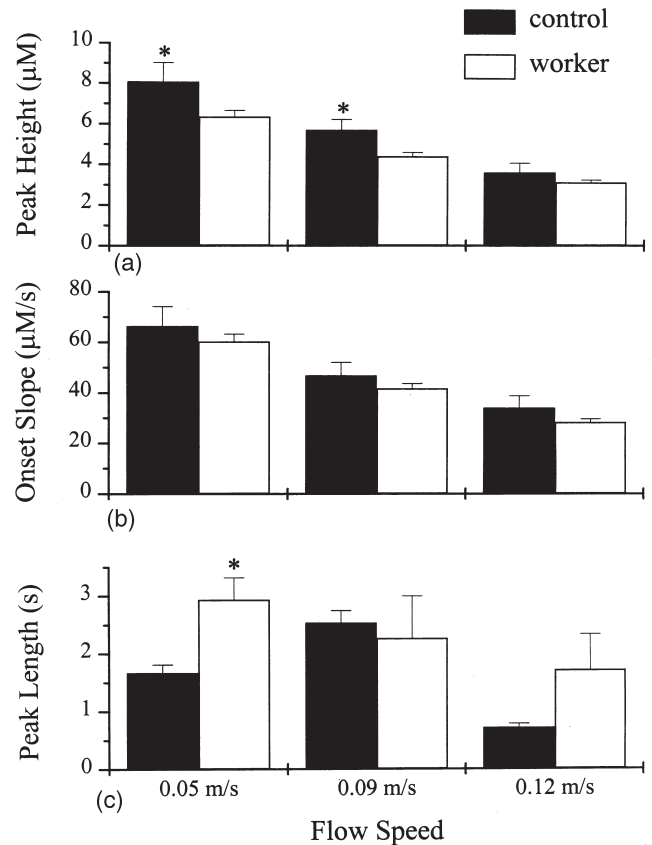


Fig. 3. Changes in pulse parameter in the boundary layer of the antenna during turbulent plume presentation. (A) Peak height for control (black bar), and worker bee antennae (white bar). (B) Onset slope for control (black bar), and worker bee antennae (white bar). (C) Length of chemical signal for control (black bar), and worker bee antennae (white bar). Points represent mean ( $\pm$  S.E.M.) for 7.6 min for five antennae. The  $t$ -test was used to determine significant difference. Asterisk (\*) indicates significant differences when compared with control  $p < 0.05$  for all tests.

slowest and intermediate flow speeds for the worker bee antennae compared to control values (Fig. 3A;  $t$ -test,  $p < 0.05$ ). The onset slope was not significantly different at the three flow speeds for the honeybee antennae when compared to control values (Fig. 3B;  $t$ -test,  $p < 0.05$ ). The peak length was significantly higher for the worker bee antennae when compared to control only at the slowest flow speed (Fig. 3C;  $t$ -test,  $p < 0.05$ ). The boundary layer around the worker bee antennae significantly alters the peak height of the environmental chemical signal and increased the length at the slowest speed.

### 3.3. Spectral analysis of odor plumes

The results of the spectral analysis of the odor signal at the slowest flow speed for the honeybee antennae shows a strong reduction in energy of the chemical signal in a narrow frequency band (0.1–2.5 Hz) (Fig. 4A). At the intermediate flow speed the spectral results show an amplification of the chemical signal of the entire odor

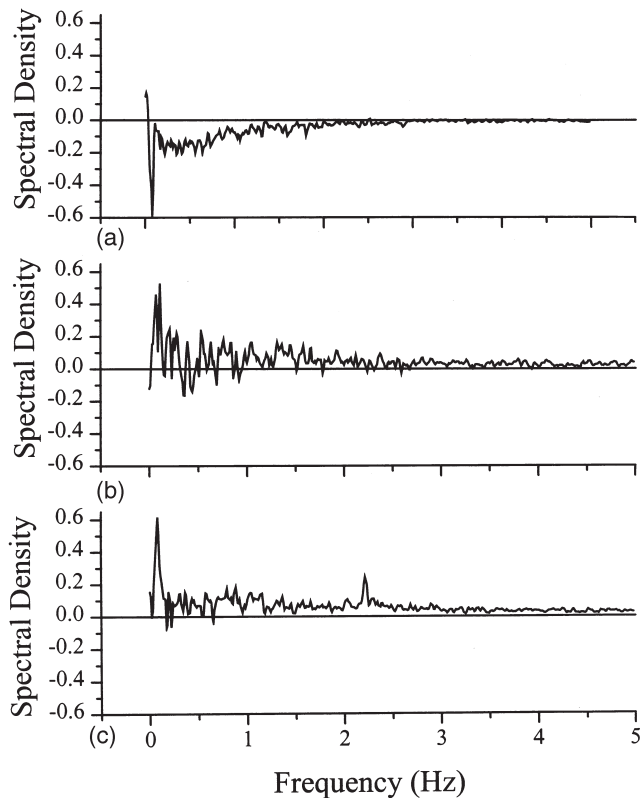


Fig. 4. Spectral density plot of the chemical signal near the worker bee antenna at the flow speed of  $0.05 \text{ m s}^{-1}$  (A),  $0.09 \text{ m s}^{-1}$  (B), and  $0.12 \text{ m s}^{-1}$  (C). Spectral plots are averages for all six bees. The difference plot was created by subtracting the spectral analysis from the control odor plumes from the spectral analysis of the boundary layer influenced odor plumes. Positive values indicates amplification of that part of the chemical spectrum, while negative value means that part of the spectrum is filtered.

plume, with the strongest amplification in the 0.1–2 Hz range (Fig. 4B). At the fastest flow speed the signal shows an amplification, with a unique amplification pattern of peaks in the 0.1 and 2.0 Hz range (Fig. 4C). This amplification is less than the amplification at the intermediate speed.

#### 4. Discussion

Our results show that the boundary layer structure determined by the morphology of the honeybee antennae significantly altered the temporal dynamics of the pulsatile chemical signal arriving at the micro-environment of the receptor cells. The onset slope of the chemical signal near the honeybee antenna was significantly increased at the slowest flow speeds (Fig. 3A). Due to the boundary layer, the decay time of the chemical signal was significantly longer near the honeybee antennae than the control signal (Fig. 2C). The pulsatile chemical signal coming into the micro-environment of the antenna was significantly slowed by the boundary layer.

The continuous signal results show that the peak height of the chemical signal significantly decreased with speed (Fig. 3). The differences in the peak height within the boundary layer of both antennae and the environmental signal suggests that the boundary layer significantly altered the spatial and temporal structure of the chemical signal perceived by the organism within a turbulent odor plume.

The results show that the boundary layer surrounding a honeybee antennae will act as a physical filter by altering the temporal and concentration dynamics of odor signals as they are transported from the environment to the receptor cells micro-environment. For honeybees, the boundary layer resulted in an amplification of the chemical signal in a broad frequency band for higher flow speeds, but dampened the signal at lower flow speeds (Fig. 4). The temporal dynamics of the chemical signal are directly due to the type of flow patterns and, to a smaller degree, the interaction of molecular diffusion and fluid flow near the antennae. The boundary layer changes flow patterns and the forces that shape the temporal structure of the chemical signal. Depending upon the exact interaction between flow and morphology, it may extract or enhance different temporal aspects of the chemical signal.

These results can be compared directly to the Schneider et al., 1997 study with the moth (*M. sexta*). That study showed that the morphology-fluid flow interaction significantly increased the peak height, onset slope and decay time. The spectral analysis showed differences in the temporal dynamics of signals recorded in the boundary layer around female and male moths. The morphology of the male and female antennae functions to extract different frequencies from the same odor plume. The moth results showed enhancement of odor fluctuations within discrete frequency bands (Schneider et al., 1997). This specific type of enhancement was completely missing from the honeybee results. It was clear that the morphology-fluid flow interaction acted as a physical filter by altering the temporal dynamics of odor signals. The differences between the spectral results from the previous study and this study can be related to the differences in antennal morphologies of the three organisms; male moth, female moth and honeybee.

Each of these organisms has many ecologically important chemical signals that are critical to reproduction. In some species of moth, the males use a point source sex pheromone plume to locate a calling female. A male's fitness is directly related to the speed and effectiveness by which it locates a female. The female moth uses odors from a host plant to locate a suitable place for oviposition. It is equally as important for other insects (i.e. honeybees), to be able to orient to a food source. It has been demonstrated empirically that the temporal dynamics of odor plumes can change even with subtle changes in the hydrodynamics (Murlis et al.,

1991; Westerberg, 1991; Moore et al., 1994). These three olfactory situations (host plant vs single female vs a single flower or patches of flowers) are drastically different in terms of the fluid dynamics that causes chemical dispersion. The difference can be demonstrated by calculating the Reynolds number for each of these situations. Each of these situations has a change in the characteristic length scale used in Reynolds number calculations which indicates the changes in flow patterns. With typical length scales, there is an order of magnitude change of the Reynolds number between a calling female, host plant and patch of flowers. As a result of the differences in signal dispersion, there will be a difference in the spatial and temporal fluctuation of chemicals within the three plumes. The differences in chemical fluctuations are also a difference in the information within the plume. Organisms with a sensory system tuned to the relevant temporal fluctuations of information in their respective environments may have a reproductive advantage. Thus, there may be a strong selection pressure for sensory properties, either physical or biological, that are tuned to the biologically relevant information within odor signals.

This idea of different amplification patterns combined with Wehner's (1987) matched filter concept, suggests that antennae morphologies can function to extract relevant information from a chemical signal. Perceiving the environment through a matched filter 'frees up the CNS from intricate computations to extract information needed for fulfilling a particular task' (Wehner, 1987). This allows the organism to remove irrelevant information arriving to the peripheral nervous system and process only relevant environmental signals. Just as receptor cells are 'spectrally-tuned' to biologically relevant chemicals within the environment, the boundary layer structure may be 'temporally tuned' to those chemical fluctuations that are most prevalent or behaviorally relevant within the environmental odor signals. Examples of physical tuning can be found in other sensory systems. Denny (1993) and Land (1981) discuss the optics of eyes and morphological differences in the relation to differences in the organism's environmental media. Denny (1993) also discusses differences in sound transmission in air and water, and the differences in physical design of auditory organs. Finally, Devarakonda et al. (1996) discusses differences in sensory performance of mechanosensory hairs in air and water. Each of these examples demonstrates how changes in the physics of signal movement result in changes in the sensory morphology. For olfaction, organisms in different sensory environments may be expected to have different antennae morphologies that act as to extract different temporal information.

Honeybees have the ability to change both their flying speed and to manipulate the orientation of the antennae (rapid vibration) with respect to flow during flight (B.H.

Smith, pers comm.). Both of these behavioral adjustments during orientation will alter the thickness and structure of the boundary layer, which in turn will change how the boundary layer alters the dynamics of incoming chemical signals. If there is sensory feedback that is connected to either the motor output that controls flight speed or antennal orientation, the honeybee may be able to control the filtering performed by the boundary layer around its antenna. This may allow the honeybee to actively 'match' the boundary layer thickness to the environmental stimulus to maximize the sensory information.

Examples of control of chemosensory input through the manipulation of physical filters have been proposed for other organisms. Crustaceans for example, can govern the boundary layer by controlling the fluid motion and boundary layer thickness around its lateral antennules. This is done by flicking their antennules (Snow, 1973), which serves to increase local fluid velocities, decrease boundary thickness and increase chemical signal transport (Moore et al., 1991). Some fish also control fluid flow over receptor appendages which allow them to control chemosensory input (Døving et al., 1977).

Although our study was done on only a single orientation, at three set flow speeds, on fully developed boundary layers, the data presented here provides a look at the spatial and temporal profile of the chemical signal near the micro-environment of the receptor cell. These results show how fluid flow around the honeybee antennae can alter the spatial and temporal dynamics that are available to receptor cells. This study can provide some insight into the structure of chemical signals as they are transported from the environment to the micro-environment around receptor cells. The interaction of fluid flow with the antenna's morphology does function as a physical filter for chemical signals. The boundary layer alters the chemical signal into a new spatial and temporal profile as it arrives to the receptor cell, this physical filter may be 'temporally tuned' to the relevant chemical signal fluctuations *A. mellifera* experience.

## Acknowledgements

This project was initiated after discussions on this topic with Dr B. H. Smith. The authors would like to thank Dr T. Keller and R.A. Zulantz for early revisions of the manuscript. This study was funded by a NSF grant to P.A.M. (NSF IBN-9614492).

## References

- Ache, B.W., 1988. Integration of chemosensory information in aquatic invertebrates. In: Atema, J., Popper, A.N., Fay, R.R., Tavolga, W.N. (Eds.), *Sensory Biology of Aquatic Animals*. Springer-Verlag, NY, pp. 29–56.

- Adam, G., Delbrück, M., 1968. Reduction of dimensionality in biological diffusion processes. In: Rich, A., Davidson, N. (Eds.), *Structural Chemistry and Molecular Biology*. W.H. Freeman, San Francisco, pp. 198–215.
- Adamson, A.W., 1973. *A Textbook of Physical Chemistry*. Academic Press, NY, p. 413.
- Borroni, P., Atema, J., 1988. Adaptation in chemoreceptor cells: I. Self-adapting backgrounds determine threshold and cause parallel shifts of response function. *Journal of Comparative Physiology A* 164, 67–74.
- Borror, D.J., Triplehorn, C.A., Johnson, N.F., 1989. *An Introduction to the Study of Insects*, 6th ed. Harcourt Brace College Publishers, NY, pp. 37–39.
- Cheer, A.Y.L., Koehl, M.A.R., 1987. Paddles and rakes: fluid flow through bristled appendages of small organisms. *Journal of Theoretical Biology* 129, 17–39.
- Denny, M.W., 1993. *Air and Water: The Biology and Physics of Life's Media*. Princeton University Press, Princeton, NJ.
- DeSimone, J.A., 1981. Physicochemical principles in taste and olfaction. In: Cagen, R.H., Kare, M.R. (Eds.), *Biochemistry of Taste and Olfaction*. Academic Press, NY, pp. 213–229.
- Devarakonda, R., Barth, F.G., Humphrey, J.A.C., 1996. Dynamics of arthropod filiform hairs. IV. Hair motion in air and water. *Philosophical Transactions of the Royal Society of London B* 351, 933–946.
- Døving, K.B., Dubois-Dauphin, M., Holley, A., Jourdan, F., 1997. Functional anatomy of the olfactory organ of fish and the ciliary mechanism of water transport. *Acta Zool.* 58, 245–255.
- Futrelle, R.P., 1984. How molecules get to their detectors: the physics of diffusion of insect pheromones. *Trends in Neuroscience* 94, 116–119.
- Gerhardt, G.A., Oke, A.F., Nagy, G., Moghaddam, B., Adams, R.N., 1984. Nafion-coated electrodes with high selectivity for CNS electrochemistry. *Brain Research* 290, 390–395.
- Gerhardt, G.A., Rose, G.M., Hoffer, B.J., 1987. *In vivo* electrochemical demonstration of potassium-evoked monoamine release from rat cerebellum. *Brain Research* 413, 327–335.
- Gleeson, R.A., Carr, W.E.S., Trapido-Rosenthal, H.G., 1993. Morphological characteristics facilitating stimulus access and removal in the olfactory organ of the spiny lobster, *Panulirus argus*: insight from the design. *Chemical Senses* 18, 67–75.
- Gomez, G., Voigt, R., Atema, J., 1994. Frequency filter properties of lobster chemoreceptor cells determined with high resolution stimulus measurement. *Journal of Comparative Physiology A* 174, 803–811.
- Land, M.F., 1981. Optics and vision in invertebrates. In: Autrum, H. (Ed.), *Invertebrate Visual Centers and Behavior: Handbook of Sensory Physiology*, vol. VII/6B. Springer-Verlag, Berlin, pp. 471–592.
- Koehl, M.A.R., 1993. Hairy little legs: feeding, smelling and swimming at low Reynolds numbers. *Contemporary Mathematics* 141, 33–64.
- Koehl, M.A.R., 1995. Fluid flow through hair-bearing appendages: feeding, smelling and swimming at low and intermediate Reynolds numbers. In: Pedley, T., Ellington, C. (Eds.), *Biological Fluid Dynamics Symp Soc. Journal of Experimental Biology*, vol. 27, pp. 157–182.
- Koehl, M.A.R., 1996. Small-scale fluid dynamics of olfactory antenna. *Marine Freshwater Behavior and Physiology* 27, 127–141.
- Moore, P.A., 1994. A model of the role of adaptation and disadaptation in olfactory receptor neurons: implications for the coding of temporal and intensity patterns of odor signals. *Chemical Senses* 19, 71–86.
- Moore, P.A., Atema, J., 1988. A model of a temporal filter in chemoreception to extract directional information from a turbulent odor plume. *Biological Bulletin* 174, 355–363.
- Moore, P.A., Atema, J., 1991. Spatial information in the three-dimensional fine structure of an aquatic odor plume. *Biological Bulletin* 181, 408–418.
- Moore, P.A., Gerhardt, G.A., Atema, J., 1989. High resolution spatio-temporal analysis of aquatic chemical signals using microelectrochemical electrodes. *Chemical Senses* 14, 829–840.
- Moore, P.A., Atema, J., Gerhardt, G.A., 1991. Fluid dynamics and microscale chemical movement in the chemosensory appendages of the lobster, *Homarus americanus*. *Chemical Senses* 16, 663–674.
- Moore, P.A., Zimmer-Faust, R.K., BeMent, S.L., Weissburg, M.J., Parrish, J.M., Gerhardt, G.A., 1992. Measurement of microscale patchiness in a turbulent aquatic odor plume using a semiconductor-based microprobe. *Biological Bulletin* 183, 138–142.
- Moore, P.A., Weissburg, M.J., Parrish, J.M., Zimmer-Faust, R.K., Gerhardt, G.A., 1994. Spatial distribution of odors in simulated benthic boundary layer flows. *Journal of Chemical Ecology* 20, 255–279.
- Murlis, J., Willis, M.A., Cardé, R.T., 1991. Odour signals: patterns in space and time. In: Døving, K. (Ed.), *Proceedings of the Tenth International Symposium on Olfaction and Taste*. Graphic Communication System, Oslo, pp. 6–17.
- Nachtigall, W., Hanauer-Thieser, U., 1992. Flight of the honeybee: drag coefficients of the bee's body; implications for flight dynamics. *Journal of Comparative Physiology B* 162, 267–277.
- Schlichting, H., 1987. *Boundary Layer Theory*. McGraw-Hill, NY.
- Schneider, R.W.S., Lanzen, J., Moore, P.A., 1997. Boundary layer effect on chemical signal movement near the antennae of the Sphinx moth, *Manduca sexta*: temporal filters for olfaction. *Journal of Comparative Physiology A* 182, 287–298.
- Snow, P.J., 1973. The antennular activities of the hermit crab *Pagurus alaskiensis* (Benedict). *Journal of Experimental Biology* 58, 745–766.
- Vogel, S., 1983. How much air passes through a silkmoth's antenna? *Journal of Insect Physiology* 29, 597–602.
- Vogel, S., 1994. *Life in Moving Fluids: The Physical Biology of Flow*, 2nd ed. Princeton University Press, Princeton, NJ.
- Wehner, R., 1987. 'Matched filters'—neural models of the external world. *Journal of Comparative Physiology A* 161, 511–531.
- Westerberg, H., 1991. Properties of aquatic odor trails. In: Døving, K. (Ed.), *Proceedings of the Tenth International Symposium on Olfaction and Taste*. Graphic Communication System, Oslo, pp. 45–65.